Solar RRL

www.solar-rrl.com

High-Performance Eight-Membered Indacenodithiophene-Based Asymmetric A-D-A Type Non-Fullerene Acceptors

Chao Li, Jiali Song, Linglong Ye, Changwoo Koh, Kangkang Weng, Huiting Fu, Yunhao Cai, Yuanpeng Xie, Donghui Wei, Han Young Woo, and Yanming Sun**

Indacenodithiophene (IDT) has been widely used as the central core to design high-performance acceptor-donor-acceptor (A-D-A)-type non-fullerene acceptors (NFAs). NFAs based on five-, six-, seven-, and nine-membered IDT have been successfully prepared. However, less research attention has been paid to the eight-membered IDT derivative. In this study, a novel asymmetric TTPTTT building block as an eight-membered IDT unit are designed and synthesized. The effect of nonfluorinated, monofluorinated, and difluorinated end-capping groups on the photovoltaic performance of TTPTTT-based NFAs are specifically investigated. By blending with the polymer donor PBT1-C, organic solar cells (OSCs) based on TTPTTT-IC, TTPTTT-2F, and TTPTTT-4F exhibited power conversion efficiencies (PCEs) of 7.91, 11.52, and 12.05%, respectively. Our results indicate that the asymmetric TTPTTT building block as an eight-membered IDT derivative is a promising central core unit for designing high-performance A-D-A type NFAs.

As a promising alternative to conventional inorganic solar cells, organic solar cells (OSCs) demonstrate great potential for harvesting solar energy and converting it to electricity in a cost-effective manner. OSCs have several distinct advantages such as their light weight, mechanical flexibility, semi-transparency, and solution processibility.[1–5] In the past decades, fullerene derivatives have played a dominant role as electron acceptors due to their high electron mobility and isotropic charge transporting properties.[6–9] However, they suffer from several inevitable drawbacks that impede their further application in OSCs, such as difficult structural modification, weak optical absorption, limited energy level variability, and unstable film morphology.[10] In recent years, non-fullerene acceptors (NFAs) with an acceptor-donor-acceptor (A-D-A) structure have drawn increasing academic and industrial research attention[11–15] and have shown great potential for further improving the photovoltaic performance of OSCs.[16–20]

With respect to the fused-ring electron-donating core (D) unit, five-membered indacenodithiophene (IDT) and its derivatives have been successfully applied for constructing high-performance A-D-A type NFAs.[21–27] For example, based on a five-membered IDT core unit, several symmetric high-performance NFAs like IDT-BOC6,[28] IEIC,[29] ATT-2,[30] and IEICO-4F[22] have been developed by introducing a π-spacer into the IDT-core-based NFAs. Very recently, we have firstly reported a novel asymmetric NFA TPTT-IC[31] using a six-membered IDT derivative (asymmetric TPTT building block) as the central core. When blended with the wide-bandgap polymer donor PBT1-C,[32] OSCs based on TPTT-IC yielded high PCE of 10.5%. In 2015, Zhan et al. designed and synthesized an ITIC acceptor using a seven-membered IDT unit as the central core.[33] Up to now, benefiting from the rational selection of polymer donor and device optimization, PCEs of ITIC-based OSCs have reached over 11%.[34] Recently, Zhan et al. have developed another non-fullerene acceptor INIC3, in which a nine-membered IDT derivative named IBDT has been employed as the core unit.[35] When blended with a FTAZ polymer donor, the device showed a high PCE of 11.5%. These results demonstrated the great success of symmetric IDT and its derivatives in designing high-performance NFAs. However, from five- to nine-membered IDT derivatives, less attention has been given to the eight-membered IDT derivative. It is thus highly desirable to develop an eight-membered IDT derivative and its corresponding A-D-A type NFAs.

The asymmetric TTPTTT building block is an eight-membered IDT derivative in which the thieno[3,2-b]thiophene (TT), phenylene (P), and dithieno[3,2-b:2′,3′-d]thiophene (TTT) moieties are condensed with two embedded cyclopentadienyl moieties. The TTPTTT unit possesses a more rigidified coplanar

C. Li, J. Song, L. Ye, K. Weng, H. Fu, Y. Cai, Y. Xie, Prof. Y. Sun
School of Chemistry
Beihang University
Beijing 100191, China
E-mail: sunym@buaa.edu.cn

C. Koh, Prof. H. Y. Woo
Department of Chemistry
College of Science
Korea University
Seoul 136-713, Republic of Korea
E-mail: hywoo@korea.ac.kr

Prof. D. Wei
The College of Chemistry and Molecular Engineering
Zhengzhou University
Zhengzhou, Henan Province 450001, China

The ORCID identification number(s) for the author(s) of this article can be found under https://doi.org/10.1002/solr.201800246.

DOI: 10.1002/solr.201800246

structure and more fused rings than the reported asymmetric TPTT unit,[31] which is beneficial for π-electron delocalization. In addition, owing to the electron donating ability of thiophene and the other thiophene units fused at each end of the TPTT building block, in principle, the TTPTTT unit has stronger electron donating ability than the TPTT unit. By comparison, in terms of the terminal electron deficient accepting (A) unit, the use of a fluorinated 1,1-dicyanomethylene-3-indanone (IC) end-capping group[15,22,36,37] has become one of the most successful approaches to design efficient A-D-A type NFAs.

The influence of fluorinated IC end-capping groups on the photovoltaic performance of NFAs has been primarily focused on symmetric core unit systems.[38] Asymmetry-core-based NFAs have been rarely studied,[31,39–41] partly because it is more challenging to synthesize and purify an asymmetric core unit than its symmetric core unit counterpart. In this study, we designed and synthesized three asymmetric NFAs (TTPTTT-IC, TTPTTT-2F, and TTPTTT-4F) using an asymmetric TTPTTT building block as the central core unit. Compared with the nonfluorinated TTPTTT-IC, the fluorinated NFAs (TTPTTT-2F and TTPTTT-4F) were found to have redshifted light absorption, downshifted molecular energy level, higher electron mobility, enhanced intramolecular charge transfer (ICT), and stronger intermolecular interactions. By blending with the wide-bandgap polymer donor PBT1-C,[32] the fluorinated NFA blend films exhibited more balanced charge transport, efficient exciton dissociation, reduced bimolecular recombination, and favorable blend morphology relative to the nonfluorinated TTPTTT-IC-based blend film. These features, along with the redshifted absorption compared to nonfluorinated TTPTTT-IC, were beneficial for obtaining higher J_{sc} and higher FF simultaneously. OSCs based on TTPTTT-2F and TTPTTT-4F exhibited PCEs of 11.52 and 12.05%, respectively, much higher than that of the nonfluorinated TTPTTT-IC counterpart (7.91%). These results demonstrate that fluorination of end-capping groups is an effective strategy to further boost the efficiency of asymmetry-core-based NFAs (**Figure 1**).

The synthesis of three NFAs is shown in **Scheme 1**. The starting material diethyl 2,5-dibromoterephthalate was subjected to Stille coupling with tributyl(thieno[3,2-b]thiophen-2-yl)stannane to afford compound 1, which was further reacted with tributyl(dithieno[3,2-b:2′,3′-d]thiophen-2-yl)stannane via Stille coupling to produce an important intermediate compound 2. Double nucleophilic addition of compound 2 with 4-hexylbenzene magnesium bromide produced two benzyl alcohols, followed by an intramolecular Friedel-Crafts cyclization to obtain a novel asymmetric TTPTTT building block. This TTPTTT unit was then reacted with n-butyllithium followed by treatment with dry DMF to furnish TTPTTT-CHO. Finally, the Knoevenagel condensation reaction of TTPTTT-CHO with nonfluorinated, monofluorinated, and difluorinated IC end-capping groups yielded the non-fullerene acceptors TTPTTT-IC, TTPTTT-2F, and TTPTTT-4F, respectively. All these intermediates and three NFAs were fully characterized using ^{1}H NMR, ^{13}C NMR, and MS (ESI†). In addition, all the NFAs have good solubility in common organic solvents such as dichloromethane, tetrahydrofuran, and chlorobenzene.

The frontier molecular orbitals and corresponding energy levels of the three TTPTTT-based NFAs, calculated by density functional theory (DFT) methods at the B97XD/6-31G level of theory, are depicted in Figure S1, Supporting Information. Introducing fluorine into the IC end-capping group has a negligible effect on the electron density distributions. For all the three TTPTTT-based NFAs, the HOMO orbitals mainly distribute in the central TTPTTT unit, whereas the LUMO orbitals are delocalized over both the central TTPTTT unit and the terminal accepting unit. The calculated HOMO/LUMO energy levels of TTPTTT-IC, TTPTTT-2F, and TTPTTT-4F are −5.43/−3.35, −5.49/−3.42, and −5.55/−3.50 eV, respectively, suggesting that incorporation of fluorine onto the IC end-capping group could lead to downshifted HOMO and LUMO energy levels. The normalized absorption spectra of the three TTPTTT-based NFAs in dilute chloroform solution and thin film

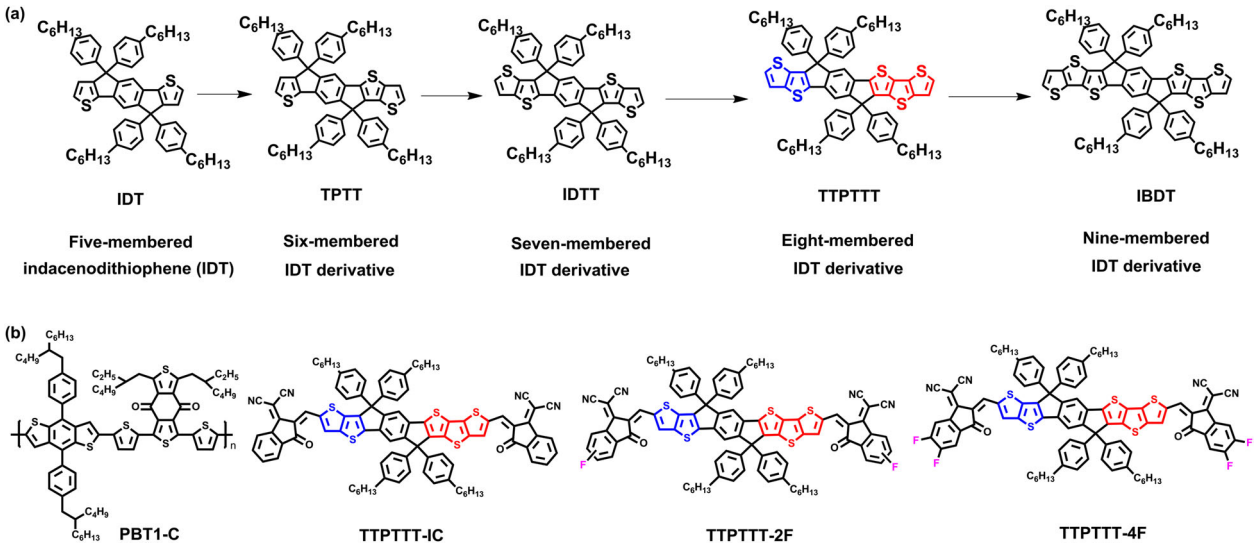

Figure 1. a) Chemical structures of IDT and its derivatives. b) Chemical structures of PBT1-C, TTPTTT-IC, TTPTTT-2F, and TTPTTT-4F.

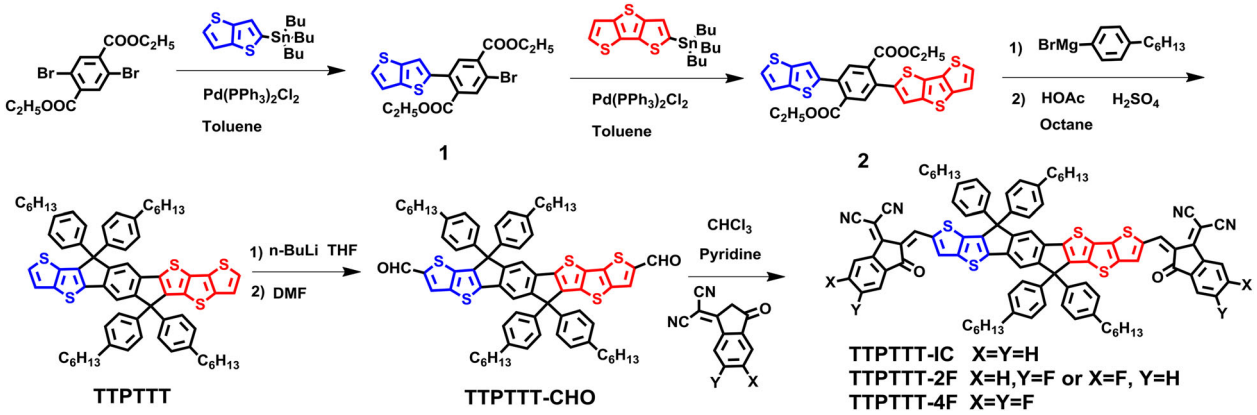

Scheme 1. Synthetic routes of TTPTTT building block and the corresponding NFAs.

are depicted in **Figure 2**. In solution, TTPTTT-IC, TTPTTT-2F, and TTPTTT-4F show maximum absorption peaks at 685, 697, and 701 nm, respectively. From solution to thin film, each NFA film exhibits a broader absorption range. Moreover, the maximum absorption peak of TTPTTT-IC, TTPTTT-2F, and TTPTTT-4F is redshifted from 685 to 700 nm, from 697 to 726 nm, and from 701 to 738 nm, respectively, indicating the presence of strong intermolecular interactions among these TTPTTT-based NFAs molecules in the solid state. It is noted that the maximum absorption peaks are redshifted both in solution and thin film as the number of fluorine atoms increases from TTPTTT-IC to TTPTTT-2F and TTPTTT-4F, suggesting that the ICT effect is enhanced after incorporating fluorine into the IC end-capping groups. The film absorption onset of TTPTTT-IC, TTPTTT-2F, and TTPTTT-4F is located at ≈777, 803, and 818 nm, which corresponds to an optical bandgap of 1.60, 1.54, and 1.52 eV, respectively. The corresponding optical data are summarized in **Table 1**.

The electrochemical properties of the TTPTTT-based NFAs were evaluated by cyclic voltammetry (CV). As shown in Figure 2c, the onset oxidation/reduction potentials of TTPTTT-IC, TTPTTT-2F, and TTPTTT-4F were measured to be 1.27/−0.50, 1.30/−0.33, and 1.32/−0.25 V, respectively. Consequently, the HOMO/LUMO energy levels of TTPTTT-IC, TTPTTT-2F, and TTPTTT-4F were calculated to be −5.64/−3.87, −5.67/−4.04, and −5.69/−4.12 eV, respectively. These

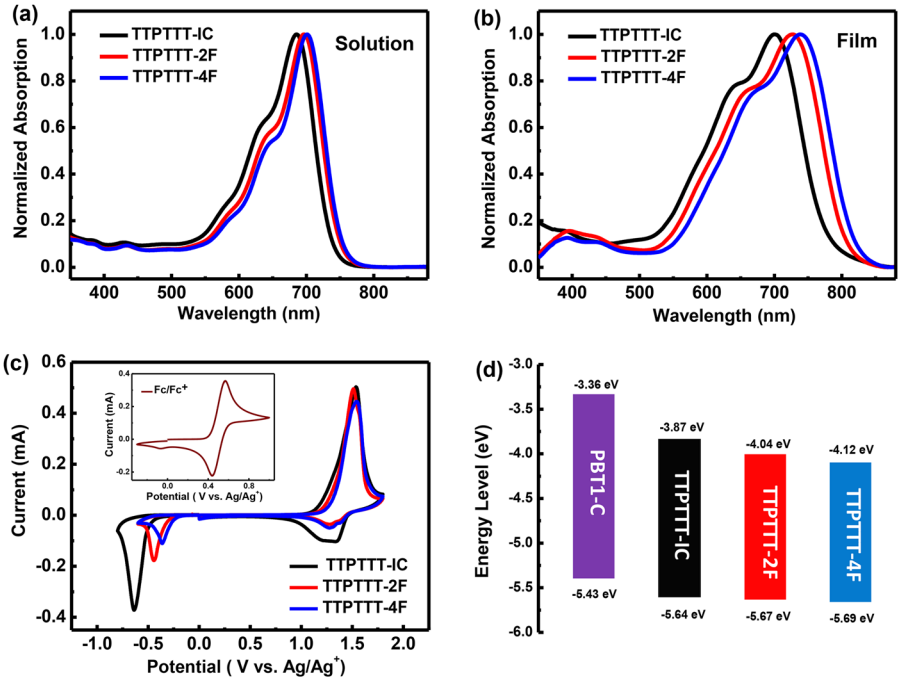

Figure 2. Absorption spectra of TTPTTT-based NFAs in (a) chloroform solution and (b) thin film; (c) cyclic voltammograms of TTPTTT-based NFAs; (d) energy level diagram of PBT1-C and TTPTTT-based NFAs.

Table 1. Optical and electrochemical data of TTPTT-based NFAs.

NFA	λ_{max}[a)] [nm]	λ_{max}[b)] [nm]	λ_{onset}[b)] [nm]	$E_g^{optc)}$ [eV]	E_{ox} [V]	HOMO [eV]	E_{red} [V]	LUMO [eV]
TTPTTT-IC	685	700	777	1.60	1.27	−5.64	−0.50	−3.87
TTPTTT-2F	697	726	803	1.54	1.30	−5.67	−0.33	−4.04
TTPTTT-4F	701	738	818	1.52	1.32	−5.69	−0.25	−4.12

[a)]In chloroform solution; [b)]in thin film drop cast from chloroform solution; [c)]estimated from the empirical formula: $E_g^{opt} = 1240/\lambda_{onset}$.

results demonstrate that both the HOMO and LUMO energy levels of fluorinated NFAs are downshifted compared with the nonfluorinated counterpart, which could be explained by the electron-withdrawing effect of fluorine.[22,42] In addition, the molecular energy levels are consistent with the results of the DFT calculations.

To evaluate the photovoltaic properties of the three TTPTTT-based NFAs, the wide-bandgap polymer donor PBT1-C was used to fabricate bulk heterojunction (BHJ) OSCs with an inverted configuration of ITO/ZnO/active layer/MoO_3/Ag, as the PBT1-C has a complementary absorption (Figure S2, Supporting Information) and appropriately matched energy levels (Figure 2) with theseTTPTTT-based NFAs. The device processing conditions, such as donor/acceptor (D/A) weight ratio, 1,8-diiodooctane (DIO) additive content[43,44], and thermal annealing temperature, were systematically optimized to obtain a maximum PCE value for each TTPTTT-based NFA BHJ blend. The *J*–*V* curves and corresponding photovoltaic data are provided in Figures S3–S5 and Tables S1–S3, Supporting Information, respectively. It was found that the optimal D/A weight ratio was 1:1.2, the optimized DIO additive content was 0.25%, and the optimal thermal annealing temperature was 100 °C. Under the aforementioned device fabrication process, the device based on TTPTTT-IC exhibited a best PCE of 7.91% with a V_{oc} of 0.996 V, J_{sc} of 12.47 mA cm^{-2}, and FF of 63.70%. The high V_{oc} approaching 1.0 V is ascribed to the large energy difference between the HOMO of PBT1-C and the LUMO of TTPTTT-IC. In comparison with the TTPTTT-IC-based device, the device based on TTPTTT-2F showed a higher PCE of 11.52%, with a V_{oc} of 0.920 V, J_{sc} of 16.78 mA cm^{-2}, and FF of 74.60%. The remarkably enhanced PCE is mainly attributed to significantly improved J_{sc} and FF values, which could be partly attributed to the redshifted absorption and enhanced charge carrier mobility of TTPTTT-2F than that of TTPTTT-IC. The slightly decreased V_{oc} of 0.920 V of the TTPTTT-2F-based device agreed well with the downshifted LUMO energy level of TTPTTT-2F relative to TTPTTT-IC. Further increasing the number of fluorine atoms from TTPTTT-2F to TTPTTT-4F resulted in a decrease of V_{oc} from 0.920 to 0.863 V. However, the device based on TTPTTT-4F achieved the highest J_{sc} (19.36 mA cm^{-2}), thus leading to the highest maximal PCE of 12.05%. The *J*–*V* curves of the optimized devices are depicted in **Figure 3**, and their corresponding optimum photovoltaic performance parameters are summarized in **Table 2**. The operational stability of the PBT1-C:TTPTTT-IC, PBT1-C:TTPTTT-2F, and PBT1-C:TTPTTT-4F devices under continuous AM1.5 illumination at 100 mW cm^{-2} was tested (Figure S6, Supporting Information). It can be seen that the stability of the devices follows the trend PBT1-C:TTPTTT-IC<PBT1-C:TTPTTT-2F<PBT1-CTTPTTT-4F, suggesting that the devices based on fluorinated NFAs show better operational stability than that of the nonfluorinated TTPTTT-IC based device.

The corresponding external quantum efficiency (EQE) spectra of the optimized devices are presented in Figure 3b. The TTPTTT-IC based device showed a broad photon response in the wavelength region from 300 to 800 nm with a maximum EQE value reaching 57.5% at 570 nm. Compared with the nonfluorinated TTPTTT-IC based device, the fluorinated TTPTTT-based devices exhibited broader photon responses and higher maximum EQE values. Specifically, the maximum EQE values of the TTPTTT-2F- and TTPTTT-4F-based devices were 72.1 and 76.9%, respectively, suggesting that the introduction of fluorinated IC end-capping groups onto asymmetric TTPTTT-cored NFAs is beneficial for highly efficient photon harvesting and charge collection. The J_{sc} values, which were calculated from integration of the EQE spectra, were 12.13, 16.38, and 18.54 mA cm^{-2} for the TTPTTT-IC-, TTPTTT-2F-, and TTPTTT-4F-based devices, respectively, which are within 5% deviation with the J_{sc} values determined from the *J*–*V* measurements.

The charge transport properties of three NFAs and their blend films were evaluated by space charge limited current (SCLC) measurements (Figure S7, Supporting Information). The neat TTPTTT-IC, TTPTTT-2F, and TTPTTT-4F film exhibited an electron mobility of 2.78×10^{-4}, 4.99×10^{-4}, and 6.49×10^{-4} cm^2 V^{-1} s^{-1}, respectively. These results demonstrate that increasing the number of fluorine atoms into the IC end-capping group is advantageous for enhancing the electron mobility of TTPTTT-based NFAs. The hole/electron mobilities of the PBT1-C:TTPTTT-IC, PBT1-C:TTPTTT-2F, and PBT1-C:TTPTTT-4F blend films were measured to be $6.43 \times 10^{-4}/1.71 \times 10^{-4}$, $3.99 \times 10^{-4}/2.64 \times 10^{-4}$, and $5.31 \times 10^{-4}/3.18 \times 10^{-4}$ cm^2 V^{-1} s^{-1}, corresponding to a μ_h/μ_e ratio of 3.76, 1.51, and 1.67, respectively. It is noteworthy that, in comparison with the blend film based on nonfluorinated TTPTTT-IC, the blend film based on fluorinated NFAs exhibited higher electron mobilities and more balanced μ_h/μ_e ratios, which favor reducing charge recombination, thus helping to achieve higher J_{sc} and FF values.

To study the exciton dissociation and charge extraction properties, the photocurrent density (J_{ph}) versus the effective voltage (V_{eff}) of the OSCs was measured. As shown in Figure 3c, for all three TTPTTT-based devices, an increased J_{ph} value could be obtained with an increase of V_{eff}. The J_{ph} value could reach saturation, J_{sat}, at high V_{eff} (>2 V), suggesting that all the photogenerated excitons could be dissociated into free charge carriers and collected by

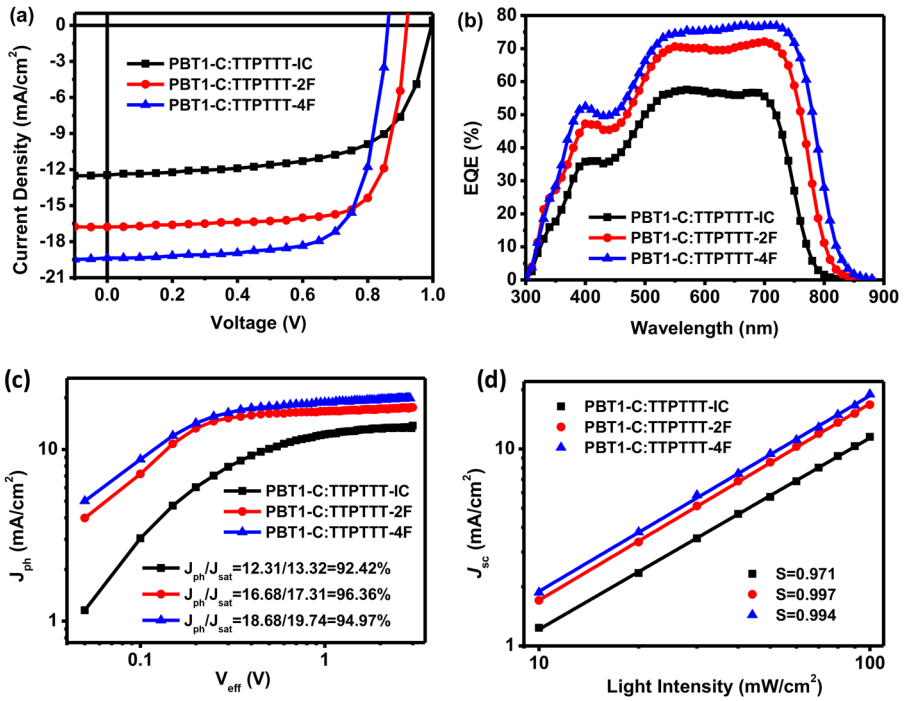

Figure 3. a) *J–V* curves and (b) the corresponding EQE spectra of OSCs based on different NFA acceptors. c) J_{ph} versus V_{eff} plot and (d) light intensity dependence of J_{sc} of the optimized devices.

electrodes. Under short-circuit conditions, compared with the nonfluorinated TTPTTT-IC-based device with a J_{ph}/J_{sat} ratio of 92.42%, the devices based on fluorinated NFAs achieved higher J_{ph}/J_{sat} ratios, with a ratio of 96.36% for the TTPTTT-2F-based device and 94.97% for the TTPTTT-4F-based device. These results demonstrate that the TTPTTT-2F-based device had the most efficient exciton dissociation and charge extraction efficiency relative to the other two devices, which could be highly desirable for achieving the highest FF. To understand the charge recombination behavior, the dependence of the photocurrent (J_{ph}) on different light intensity (P_{light}) was also measured. The relationship between J_{sc} and P_{light} can be described by the formula $J_{sc} \propto P_{light}^{S}$, where the exponential factor S is an indicator of the extent of bimolecular recombination. As depicted in Figure 3d, the S values of the TTPTTT-IC-, TTPTTT-2F-, and TTPTTT-4F-based devices were calculated to be 0.971, 0.997, and 0.994, respectively, implying that negligible bimolecular recombination occurred in all three blend devices.

To investigate the morphologies of the three TTPTTT-based blend films, atomic force microscopy (AFM) was performed. As shown in **Figure 4**, compared with the nonfluorinated TTPTTT-IC-based blend film, the fluorinated NFAs blend films not only exhibited a more obvious fibrous structure, but also presented smaller root-mean-square (RMS) roughness, with a RMS value of 1.46 and 1.26 nm for the TTPTTT-2F and TTPTTT-4F blend films, respectively. From the AFM phase images, it can be seen clearly that all three blend films exhibited a fibril network morphology, which is beneficial for efficient charge transport in the OSC devices.

To better understand the molecular orientation and packing behavior in neat and blend films, grazing incidence wide angle X-ray scattering (GIWAXS) measurements were carried out. The 2D GIWAXS images and corresponding line-cuts are presented in **Figure 5**. As evidenced by the strong (100) and (010) scattering peaks in the in-plane (IP) and out-of-plane (OOP) direction, respectively, all three NFA neat films are interpreted to prefer to adopt a face-on orientation relative to the substrate. However, there exists a distinct difference in the IP and OOP line-cut profiles (Figure 5b). In the IP direction, the scattering intensity of the (100) lamellar stacking peak in pristine film increases and the crystal coherence length (CCL) based on the full width at half

Table 2. Photovoltaic data of OSCs based on different NFA acceptors.

NFA	V_{oc} [V]	J_{sc} [mA cm^{-2}]	$J_{sc,cal}$ [mA cm^{-2}]	FF [%]	PCE[a)] [%]
TTPTTT-IC	0.996 (0.992 ± 0.006)	12.47 (12.26 ± 0.20)	12.13	63.7 (63.04 ± 0.60)	7.91 (7.69 ± 0.22)
TTPTTT-2F	0.920 (0.92 ± 0.004)	16.78 (16.67 ± 0.14)	16.38	74.60 (73.48±0.81)	11.52 (11.21 ± 0.22)
TTPTTT-4F	0.863 (0.861 ± 0.005)	19.36 (19.29 ± 0.17)	18.54	72.10 (71.23 ± 0.63)	12.05 (11.89 ± 0.14)

[a)]Average values with standard deviation were obtained from 20 devices.

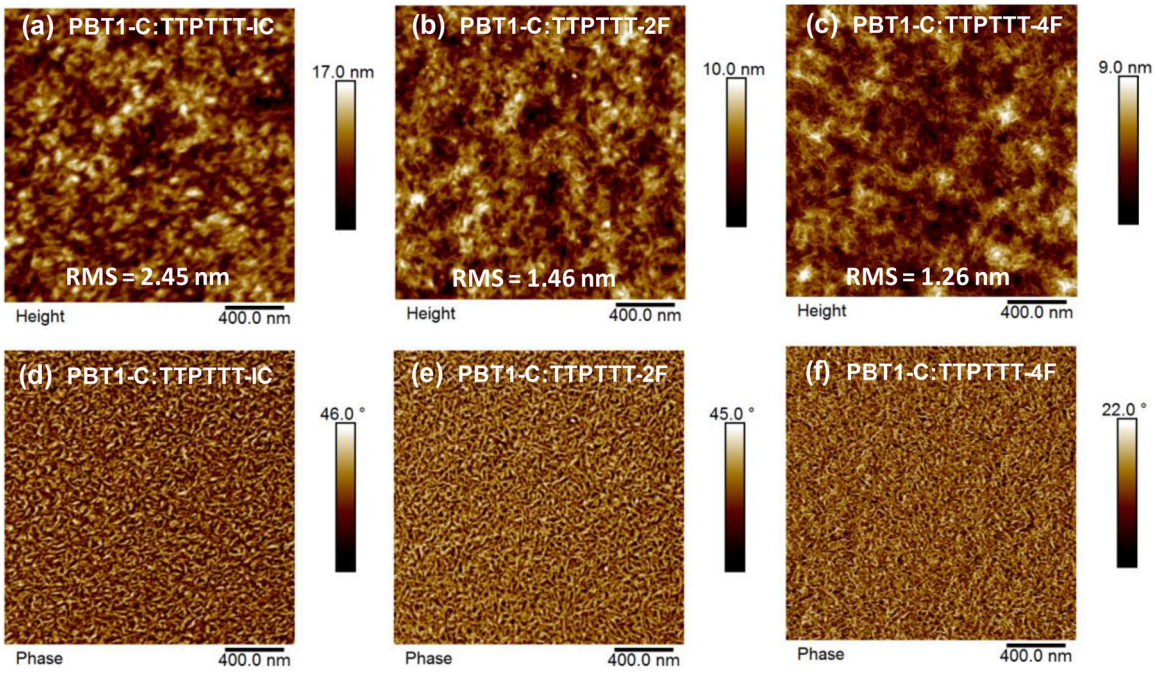

Figure 4. AFM height images (a–c) and phase images (d–f) of PBT1-C:NFA blend films.

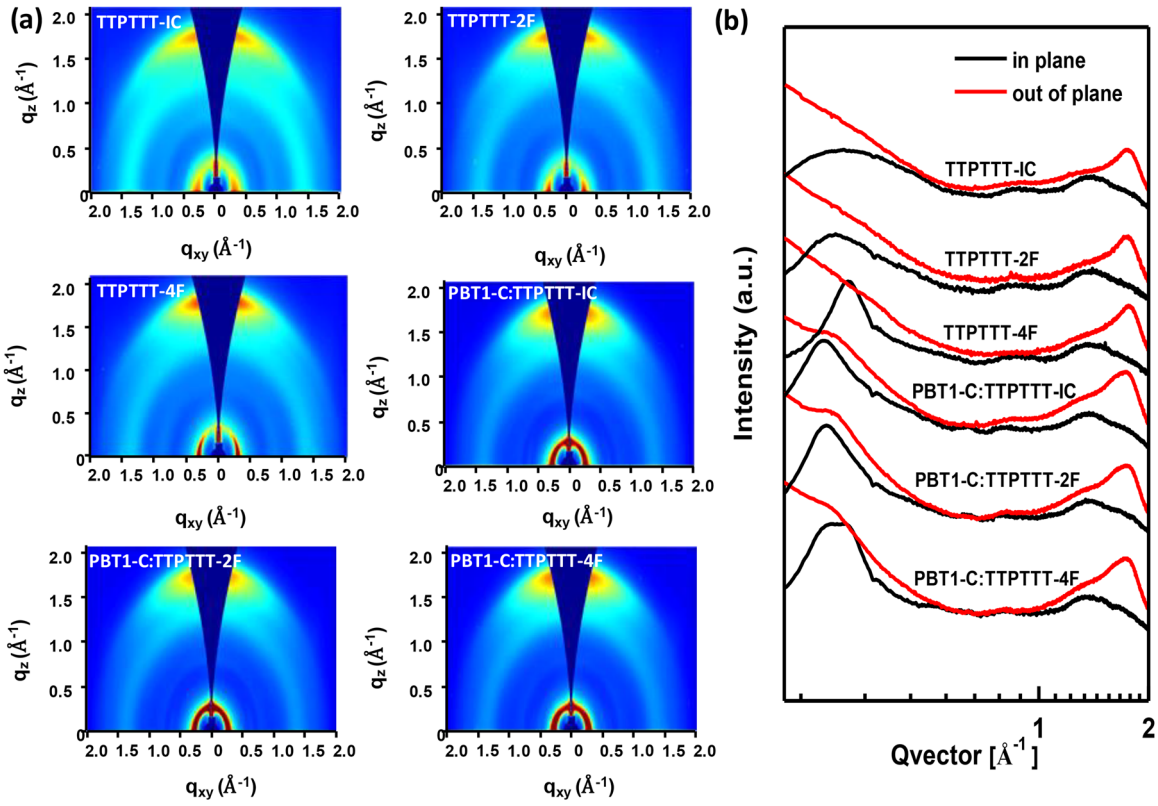

Figure 5. a) Grazing incidence wide angle X-ray diffraction patterns (GIWAXS) of TTPTTT-IC, TTPTTT-2F, TTPTTT-4F, and their corresponding blend films. b) In-plane (black lines) and out-of-plane (red lines) line-cut profiles of the neat and blend films.

maximum of the IP (100) peak increases in sequence from TTPTTT-IC (27.8 Å) to TTPTTT-2F (48 Å) and to TTPTTT-4F (98.2 Å), indicating that incorporating fluorine onto the IC end-capping group increases the molecular ordering of NFAs, which is desirable for achieving high electron mobility. Moreover, in the OOP direction, the tightest π-π stacking was measured for the TTPTTT-4F film with a d-spacing of 3.54 Å, showing a stronger cofacial intermolecular packing with fluorine substituents. When blended with PBT1-C, the predominant face-on orientation maintains in all the blend films, which is beneficial for vertical charge transport in OSC devices. Associated with the (100) lamellar stacking peak of 0.26 $Å^{-1}$ originated from PBT1-C and the (010) diffraction peak of the TTPTTT-based NFAs in the OOP direction, both the polymer donor PBT1-C (Figure S8, Supporting Information) and the TTPTTT based NFAs are expected to maintain their respective molecular ordering in the blend films, which contributes to the achieved high hole and electron mobilities in the blends.

In summary, based on an eight-membered IDT derivative, termed the TTPTTT building block, we have designed and synthesized three novel asymmetric non-fullerene acceptors (TTPTTT-IC, TTPTTT-2F, and TTPTTT-4F), to investigate the effect of nonfluorinated, monofluorinated, and difluorinated IC end-capping groups on the electronic and photovoltaic properties of asymmetry-core-based non-fullerene acceptors. The incorporation of fluorinated IC end-capping groups led to redshifted light absorption, downshifted molecular energy levels, improved electron mobility, and strong intramolecular/intermolecular interactions. By employing the PBT1-C polymer donor, OSCs based on fluorinated NFAs exhibited significantly higher J_{sc} and FF values than their nonfluorinated TTPTTT-IC counterpart. Consequently, high PCEs of 11.52 and 12.05% were achieved for TTPTTT-2F- and TTPTTT-4F-based devices, respectively, which are much higher than that of the TTPTTT-IC device (7.91%). Our study not only indicates that the TTPTTT building block as an eight-membered IDT derivative is a promising central core for designing high-performance A-D-A-type non-fullerene acceptors, but also demonstrates that fluorination of the IC end-capping group is an effective strategy to further boost the PCE of asymmetry-core-based NFAs.

Supporting Information

Supporting Information is available from the Wiley Online Library or from the author.

Acknowledgements

C.L. and J.S. contributed equally to this work. This work was financially supported by the National Natural Science Foundation of China (NSFC) (No. 21734001, 51473009, 21674007). H.Y.W. acknowledges the financial support from National Research Foundation (NRF) of Korea (2012M3A6A7055540, 2015M1A2A2057506).

Conflict of Interest

The authors declare no conflict of interest.

Keywords

asymmetric non-fullerene acceptor, indacenodithiophene derivative, organic solar cells, power conversion efficiency

Received: September 5, 2018
Revised: October 2, 2018
Published online: October 26, 2018

[1] Y. Cai, L. Huo, Y. Sun, *Adv. Mater.* **2017**, *29*, 1605437.
[2] G. Li, R. Zhu, Y. Yang, *Nat. Photonics* **2012**, *6*, 153.
[3] Y.-J. Cheng, S.-H. Yang, C.-S. Hsu, *Chem. Rev.* **2009**, *109*, 5868.
[4] L. Lu, T. Zheng, Q. Wu, A. M. Schneider, D. Zhao, L. Yu, *Chem. Rev.* **2015**, *115*, 12666.
[5] Y.-W. Su, S.-C. Lan, K.-H. Wei, *Mater. Today* **2012**, *15*, 554.
[6] S. Günes, H. Neugebauer, N. S. Sariciftci, *Chem. Rev.* **2007**, *107*, 1324.
[7] J. Zhao, Y. Li, G. Yang, K. Jiang, H. Lin, H. Ade, W. Ma, H. Yan, *Nat. Energy* **2016**, *1*, 15027.
[8] J. Ren, Y. Zhang, F. Liu, Y. Yan, M. Qiu, V. A. L. Roy, H. Zheng, M. Sun, R. Yang, *RSC Adv.* **2016**, *6*, 68049.
[9] Y.-W. Su, Y.-C. Lin, K.-H. Wei, *J. Mater. Chem. A* **2017**, *5*, 24051.
[10] Y. Lin, X. Zhan, *Mater. Horiz.* **2014**, *1*, 470.
[11] G. Zhang, J. Zhao, P. C. Y. Chow, K. Jiang, J. Zhang, Z. Zhu, J. Zhang, F. Huang, H. Yan, *Chem. Rev.* **2018**, *118*, 3447.
[12] J. Hou, O. Inganäs, R. H. Friend, F. Gao, *Nat. Mater.* **2018**, *17*, 119.
[13] Y. Ma, M. Zhang, Y. Yan, J. Xin, T. Wang, W. Ma, C. Tang, Q. Zheng, *Chem. Mater.* **2017**, *29*, 7942.
[14] X. Shi, J. Chen, K. Gao, L. Zuo, Z. Yao, F. Liu, J. Tang, A. K. Y. Jen, *Adv. Energy Mater.* **2018**, *8*, 1702831.
[15] J. Sun, X. Ma, Z. Zhang, J. Yu, J. Zhou, X. Yin, L. Yang, R. Geng, R. Zhu, F. Zhang, W. Tang, *Adv. Mater.* **2018**, *30*, 1707150.
[16] C. Yan, S. Barlow, Z. Wang, H. Yan, A. K. Y. Jen, S. R. Marder, X. Zhan, *Nat. Rev. Mater.* **2018**, *3*, 18003.
[17] C. B. Nielsen, S. Holliday, H.-Y. Chen, S. J. Cryer, I. McCulloch, *Acc. Chem. Res.* **2015**, *48*, 2803.
[18] N. Liang, W. Jiang, J. Hou, Z. Wang, *Mater. Chem. Front.* **2017**, *1*, 1291.
[19] P. Cheng, G. Li, X. Zhan, Y. Yang, *Nat. Photonics* **2018**, *12*, 131.
[20] J. Zhu, Y. Xiao, J. Wang, K. Liu, H. Jiang, Y. Lin, X. Lu, X. Zhan, *Chem. Mater.* **2018**, *30*, 4150.
[21] S. Li, L. Ye, W. Zhao, S. Zhang, S. Mukherjee, H. Ade, J. Hou, *Adv. Mater.* **2016**, *28*, 9423.
[22] H. Yao, Y. Cui, R. Yu, B. Gao, H. Zhang, J. Hou, *Angew. Chem. Int. Ed.* **2017**, *56*, 3045.
[23] S. Yu, Y. Chen, L. Yang, P. Ye, J. Wu, J. Yu, S. Zhang, Y. Gao, H. Huang, *J. Mater. Chem. A* **2017**, *5*, 21674.
[24] T. J. Aldrich, S. M. Swick, F. S. Melkonyan, T. J. Marks, *Chem. Mater.* **2017**, *29*, 10294.
[25] R. Li, G. Liu, M. Xiao, X. Yang, X. Liu, Z. Wang, L. Ying, F. Huang, Y. Cao, *J. Mater. Chem. A* **2017**, *5*, 23926.
[26] M. Chang, Y. Wang, Y.-Q. -Q. Yi, X. Ke, X. Wan, C. Li, Y. Chen, *J. Mater. Chem. A* **2018**, *6*, 8586.
[27] J. Song, C. Li, L. Ye, C. Koh, Y. Cai, D. Wei, H. Woo, Y. Sun, *J. Mater. Chem. A* **2018**, *6*, 18847.
[28] Y. Liu, Z. Zhang, S. Feng, M. Li, L. Wu, R. Hou, X. Xu, X. Chen, Z. Bo, *J. Am. Chem. Soc.* **2017**, *139*, 3356.
[29] Y. Lin, Z.-G. Zhang, H. Bai, J. Wang, Y. Yao, Y. Li, D. Zhu, X. Zhan, *Energy Environ. Sci.* **2015**, *8*, 610.
[30] F. Liu, Z. Zhou, C. Zhang, J. Zhang, Q. Hu, T. Vergote, F. Liu, T. P. Russell, X. Zhu, *Adv. Mater.* **2017**, *29*, 1606574.

[31] C. Li, Y. Xie, B. Fan, G. Han, Y. Yi, Y. Sun, *J. Mater. Chem. C* **2018**, *6*, 4873.
[32] T. Liu, L. Huo, S. Chandrabose, K. Chen, G. Han, F. Qi, X. Meng, D. Xie, W. Ma, Y. Yi, J. M. Hodgkiss, F. Liu, J. Wang, C. Yang, Y. Sun, *Adv. Mater.* **2018**, *30*, 1707353.
[33] Y. Lin, J. Wang, Z.-G. Zhang, H. Bai, Y. Li, D. Zhu, X. Zhan, *Adv. Mater.* **2015**, *27*, 1170.
[34] W. Zhao, D. Qian, S. Zhang, S. Li, O. Inganäs, F. Gao, J. Hou, *Adv. Mater.* **2016**, *28*, 4734.
[35] S. Dai, F. Zhao, Q. Zhang, T.-K. Lau, T. Li, K. Liu, Q. Ling, C. Wang, X. Lu, W. You, X. Zhan, *J. Am. Chem. Soc.* **2017**, *139*, 1336.
[36] F. Zhao, S. Dai, Y. Wu, Q. Zhang, J. Wang, L. Jiang, Q. Ling, Z. Wei, W. Ma, W. You, C. Wang, X. Zhan, *Adv. Mater.* **2017**, *29*, 1700144.
[37] W. Liu, J. Zhang, Z. Zhou, D. Zhang, Y. Zhang, S. Xu, X. Zhu, *Adv. Mater.* **2018**, *30*, 1800403.
[38] B. Kan, J. Zhang, F. Liu, X. Wan, C. Li, X. Ke, Y. Wang, H. Feng, Y. Zhang, G. Long, R. H. Friend, A. A. Bakulin, Y. Chen, *Adv. Mater.* **2018**, *30*, 1704904.
[39] S. Feng, C. Zhang, Y. Liu, Z. Bi, Z. Zhang, X. Xu, W. Ma, Z. Bo, *Adv. Mater.* **2017**, *29*, 1703527.
[40] W. Zhai, A. Tang, B. Xiao, X. Wang, F. Chen, E. Zhou, *Sci. Bull.* **2018**, *63*, 845.
[41] W. Gao, M. Zhang, T. Liu, R. Ming, Q. An, K. Wu, D. Xie, Z. Luo, C. Zhong, F. Liu, F. Zhang, H. Yan, C. Yang, *Adv. Mater.* **2018**, *30*, 1800052.
[42] F. Yang, C. Li, W. Lai, A. Zhang, H. Huang, W. Li, *Mater. Chem. Front.* **2017**, *1*, 1389.
[43] M.-S. Sun, C.-Y. Kuo, M.-C. Yuan, U.-S. Jeng, C.-J. Su, K.-H. Wei, *Adv. Mater.* **2011**, *23*, 3315.
[44] C.-M. Liu, Y.-W. Su, J.-M. Jiang, H.-C. Chen, S.-W. Lin, C.-J. Su, U. S. Jeng, K.-H. Wei, *J. Mater. Chem. A* **2014**, *2*, 20760.